MULTI-CHARGED IONS SOURCE

L.S. Glazunov, A.V. Zats, S.G. Karpus, V.V. Kuz'menko, V.M. Pistryak*

National Science Center "Kharkov Institute of Physics and Technology", 61108, Kharkov, Ukraine

(Received April 12, 2011)

The multi-charged ion source (MCIS) with high voltage Penning discharge and end extraction was developed. The bench tests of ion source were made, the operation parameters and initial characteristics of extracted beam were determined. It was shown that MCIS operation parameters and ion beam characteristics are satisfied to exploitation conditions on the "SOKOL" accelerator.

PACS: 07.77.Ka

INTRODUCTION

The multi-charged ion acceleration on the "SOKOl" accelerator gives possibility to extend the analytical properties and increase ion energy range of the "SOKOL" facility[1]. E.g. the using doubly charged ions of helium can provides:

- elastic recoil detection method in the solid state targets for the hydrogen concentration, obtaining the concentration profile of a hydrogen by depth;
- studding oxide layers by RBS-method using ions of He^{++} with energy $3.6\,MeV$ using resonance elastic backscattering at $3.047\,MeV$; research of isotope content thin films of magnesium and silicon targets; multi-layer structure.

The multi-charged ion sources (MCIS) are widely using at the charge particles accelerators of different types (electrostatic accelerators, cyclotrons, linear accelerators), which have scientific and industrial application. Currently many MCIS$'$s were developed[2]:

- gas plasma discharge MCIS;
- EBIS (ion source with electron beam);
- ECR (resonance microwave discharge);
- LIS (laser ion sources).

Developing of MCIS the main attention was paid for raising charge state producible ions and corresponding to all requirements which connected with specific accelerator exploitation. The main process to get multi-charged ions is electron impact ionization. The cross-sections of ion-atom collisions is less than cross-section of electron-atom collisions and can be neglected. The production of multi-charged ions runs through two phases: single-step ionization and multi-step one. The single-step ionization of multi-charged ion production is the result of single collision of electron with the atom. The multi-step ionization of multi-charged ion production arises if electron has several collisions with the atom. The magnitudes of electron impact ionizations depend on electrons energy [3]. Along with processes of multi-charged ion production the loss charge processes take place. The processes are electron-ion collisions, atom-ion collisions and the collision of ion-ion. The main process which causes reducing of charge state is the ion-atom collision. Reasoning from the analysis of multi-charged ion production and their charge loss, we can formulate the main requirements for MCIS, which it must to satisfy:

- the presence of high energy electrons which can ionize the atoms to the high charge states and high density of high energy electrons;
- the maximum possible multiplication value of electron density and time the plasma holds ions;
- the low density of the neutral atoms to decreasing charge states losses by multi-charged ions in the ion-atom collisions.

MCIS CONSTRUCTION

Besides the list of requirements for MSIC which was mentioned in previous part of paper we have special requirements which connected with its accelerator exploitation. The ion source for "SOKOL" accelerator must meet the following requirements:

- the low operation gas flow ($Q < 10^{-4}\,m^3\,Pa/s$) provides high vacuum in the accelerating tube;
- the power consumption must be less than $150\,W$;
- the ion source's weight is about $4...5\,kg$, because the mechanical strength of accelerating tube is limited and ion source dimensions must be small for its free location in the high voltage terminal;

*Corresponding author E-mail address: karpus@kipt.kharkov.ua

– the simplicity of operation;

– the ion source lifetime is more than 150 *hours*.

The reference analysis gave a possibility to make a conclusion that Penning type ion source with high voltage gaseous discharge with cold cathodes and axial ion extraction satisfies the requirements [4,5].

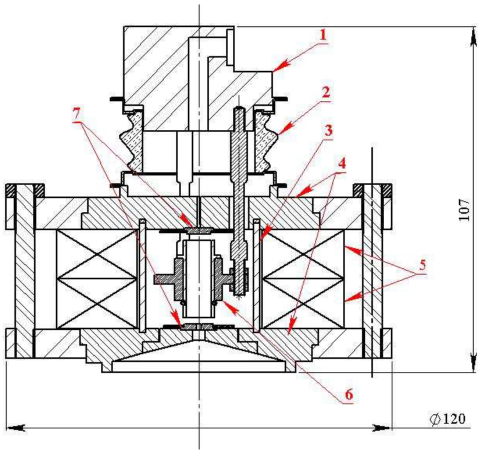

Fig.1a. *The scheme of the MCIS. 1 - the anode flange, 2 - the insulator, 3 - the case cylinder (12Cr18Ni10Ti steel), 4 - the cathode flanges (soft magnetic steel), 5 - the permanent magnets, 6 - the cylindrical anode, 7 - the cathodes. (All sizes are in mm)*

Hence the new ion source construction was developed, which is presented in the Fig.1 (1a. and 1b.). The ion source case is consisted of the cathodes flange (4) and case cylinder (3). The cathode flanges are connected with each other by the nonmagnetic cap flanges and is tightened with studs. The tantalum cathodes (7) are mounted on the cathodes flanges. The molybdenum anode (6) of the ion source connected with the anode flange (1) with three studs.

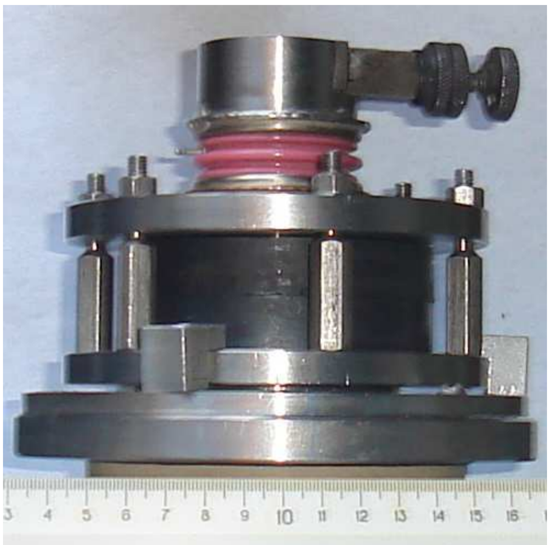

Fig.1b. *The appearance of the MCIS*

The homogeneous magnetic field in the discharge chamber is producing by permanent magnets (5) and the cathode flanges (4). To choose optimal diameter of soft magnetic flanges for maximum production of magnetic induction the modeling of magnetic system was realized and distribution of magnetic induction along the axis symmetry of ion source and its value for different diameters of flange was measured.

THE MCIS BENCH TESTS

To detect the optimal parameters of MCIS and study initial characteristics of ion beam that need for developing the injection system the bench tests were made. Operation gases for MCIS bench tests were neon, argon and helium. The Fig.2 shows the functions of discharge current (I_d) and extracted total ion beam (I_t) depending on difference of potentials between "anode-cathode" when gas flow was constant.

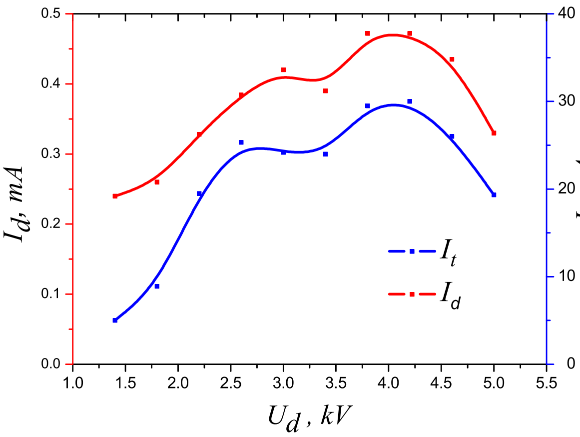

Fig.2. *The discharge current I_d and total ion current I_t versus discharge voltage U_d, the extraction voltage was $U_{extr} = 8\,kV$ and neon flow was $Q = 3.9 \cdot 10^{-5}\,m^3Pa/s$*

As was shown in the Fig.2 the curves have two peaks: the first for discharge voltage $U_d \approx 2.8\,kV$ and the second for $U_d \approx 4.2\,kV$. The same functions was observed by authors [4,5]. This effect can be explained by the presence of optimal parameters for glow discharge, which are determined as a ratio of discharge voltage (U_d), pressure of operation gas (gas flow Q) and magnetic induction B. In the Fig.3 (A,B) the function of discharge current and extracted ion beam currents with respect to gas flow is shown for the constant anode potential, which is correspond to two current maxima shown in the Fig.2. These functions indicate that with operation gas flow increasing, ion beam and discharge currents are increasing too when anode potential keeps the same value. The main MCIS characteristic is charge state distribution of extracted beam. In the Fig.4 the multi-charged ion currents of neon versus of discharge voltage (potential between "anode cathode") from one of the regimes is displayed. One can see these functions are similar to functions of I_d and I_t from discharge voltage (U_d) (see Fig.2). The identical research was made when operation gas was argon (Figs.5, 6).

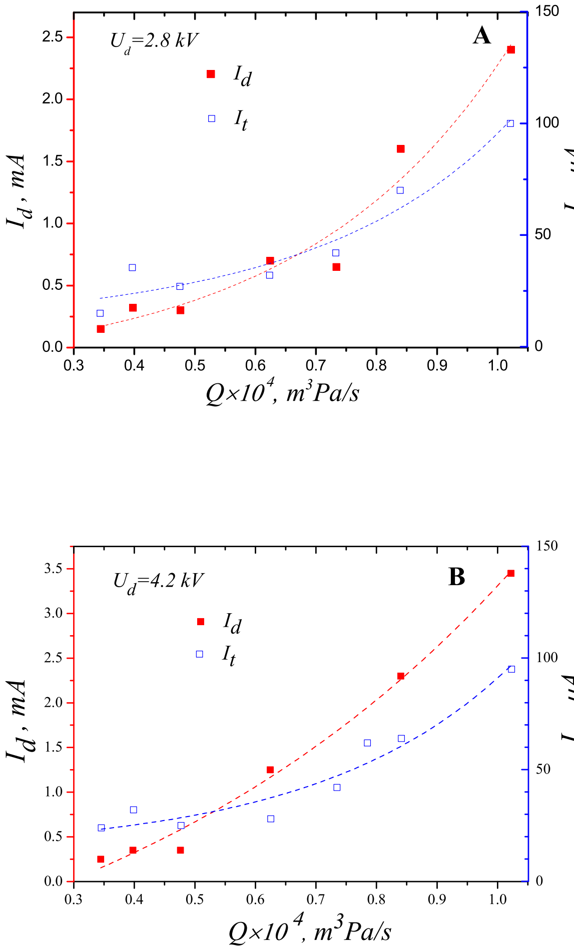

Fig.3. *The discharge current I_d and extracted ion current I_t versus gas flow Q when extraction voltage was $U_{extr} = 11\,kV$*

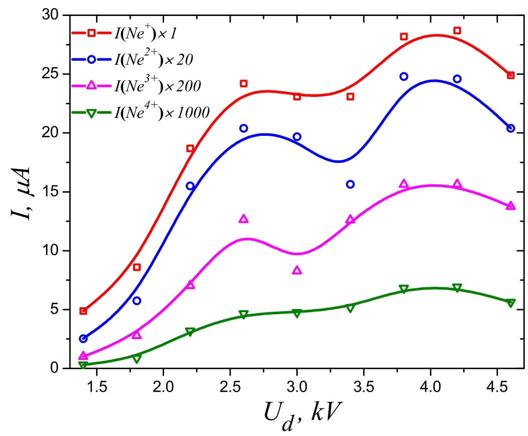

Fig.4. *The ion currents of (Ne^+, Ne^{2+}, Ne^{3+}, Ne^{4+}) versus discharge voltage U_d, when extraction potential was $U_{extr} = 8\,kV$ and neon flow was $Q = 3.9 \cdot 10^{-5}\,m^3Pa/s$*

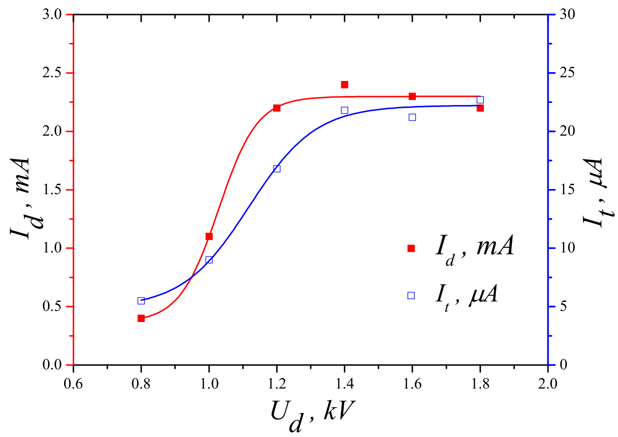

Fig.5. *The discharge and total ion currents versus of discharge voltage U_d when extracted potential was $U_{extr} = 8\,kV$ and argon flow was $Q = 1.67 \cdot 10^{-5}\,m^3Pa/s$*

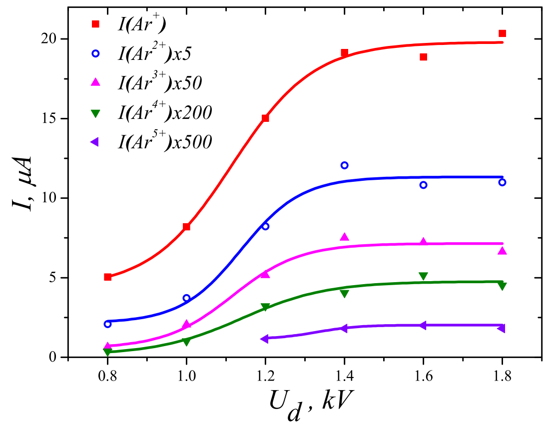

Fig.6. *The ion currents of (Ar^+, Ar^{2+}, Ar^{3+}, Ar^{4+}, Ar^{5+}) versus discharge voltage U_d, when extraction potential was $U_{extr} = 8\,kV$ and argon flow was $Q = 1.67 \cdot 10^{-5} m^3Pa/s$*

As it was mentioned above the multi-charged ion production has two phases: single-step and multi-step. The Fig.7 and Fig.8 show experimentally obtained relative outputs of multi-charged ions for given ion source and cross-sections of single step ionization at electron impact for argon versus of the charge state of ion [6]. These functions show that the main production process of multi-charged ions is the single electron-atom collision.

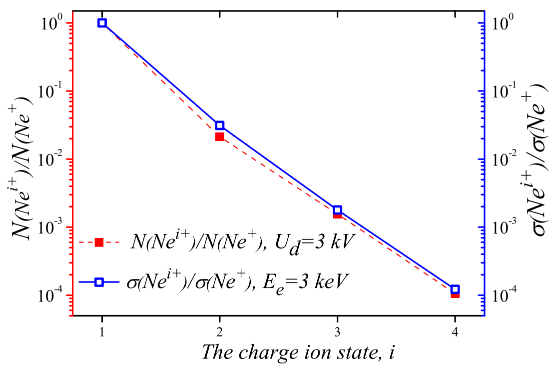

Fig.7. *The comparison of neon multi-charged ion output ratio and neon ionization cross-section ratio of single step ionization for electrons energy* $E_e = 3\,keV$

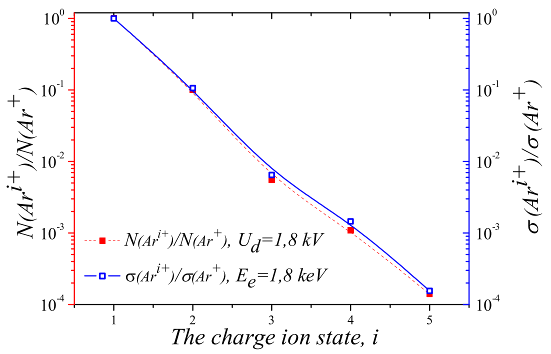

Fig.8. *The comparison of argon multi-charged ion output ratio and argon ionization cross-section ratio of single step ionization for electrons energy* $E_e = 1.8\,keV$

The neon, argon and helium ions output ratios which found during bench test and results of other authors, which had used with the same ion sources type are presented in the Table 1.

Table 1. *Relative output of extracted multi-charged ions*

Gas	Neon	Argon	Helium	Ref.
A^{2+}/A^+	$0.43{\cdot}10^{-1}$	$1.15{\cdot}10^{-1}$	$4.3{\cdot}10^{-3}$	*
	$0.7{\cdot}10^{-1}$	$1{\cdot}10^{-1}$	$5.5{\cdot}10^{-3}$	[4]
	$1.2{\cdot}10^{-1}$	$1.38{\cdot}10^{-1}$	$4.3{\cdot}10^{-3}$	[5]
A^{3+}/A^+	$2.7{\cdot}10^{-3}$	$0.7{\cdot}10^{-2}$	-	*
	$4{\cdot}10^{-3}$	$1.2{\cdot}10^{-2}$	-	[4]
	$6.45{\cdot}10^{-3}$	$1.3{\cdot}10^{-2}$	-	[5]
A^{4+}/A^+	$2.4{\cdot}10^{-4}$	$1.8{\cdot}10^{-3}$	-	*
	$1.4{\cdot}10^{-4}$	$2.3{\cdot}10^{-3}$	-	[4]
	-	-	-	[5]
A^{5+}/A^+	-	$3.45{\cdot}10^{-4}$	-	*
	-	$2.1{\cdot}10^{-4}$	-	[4]
	-	-	-	[5]

* - *present work.*

The existing differences of multi-charged ion outputs can be explained by different operation regimes of multi-charged ion sources (discharge voltage, gas flow, and magnetic induction) and ion source geometries. Hence, the results of bench tests show that technical characteristics of given multi-charged ion source (like ion beam current, multiply charged ion output, gas flow value, power consumption, dimensions and weight) are in general agreement of exploitation conditions on the "SOKOL" electrostatic accelerator.

THE INITIAL ION BEAM CHARACTERISTICS RESEARCH

One of the main characteristics of MCIS ion beam are divergence angle and ion energy spread. Such data are necessary for developing of ion beam characteristics agreement system with ion optic properties of accelerating tube. The following points were researched in this work:

- the dependence of diameter (inside given distance from emission hole) and divergence angle of ion beam on extraction potential for optimal operation regimes of ion source;
- the dependence of ion beam energy spectra on such operation parameters of the ion source:
  - discharge voltage,
  - value of gas flow,
  - type of gas.

To detect the diameter and divergence angle of ion beam the measurements of ion beam density profiles in two planes at different distances from emission hole were realized. The ion beam density profiles were measured with a mobile Faraday cup with input aperture of $1\,mm$. The principal scheme of measuring of ion beam density profile is presented in the Fig.9.

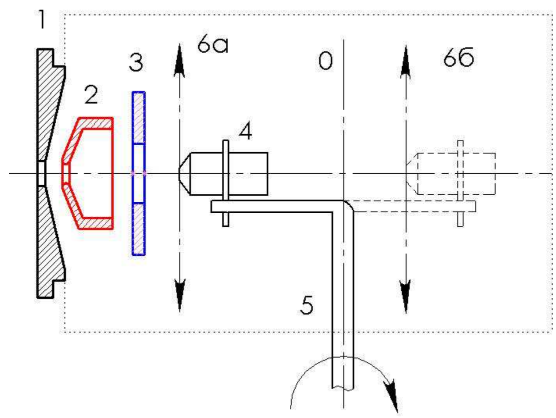

Fig.9. *The principal scheme of measuring of ion beam density profile. 1 - the cathode flange of MCIS, 2 - extraction electrode, 3 - diaphragm with aperture* $10\,mm$*, 4 - the Faraday cup, 5 - the rod, 6a and 6b - measuring planes of ion beam density profile*

The diaphragm 3 (see Fig.3) was cut a part of ion beam which had large divergence angles. At the same time the total current was decreased about 18%. The ion beam density profile versus ion beam radius when the difference of "cathode-extractor" potentials was equal to $11\,kV$ is shown in the Fig.10, these profiles was measured for two distances (125 and $274\,mm$) from emission hole. Integrating these functions one can receive the functions of ion current versus ion beam radius (see Fig.11). After plotting of these dependence in the relative units one can determine the ion beam radius for given part of ion current and maximum divergence angle of ion beam.

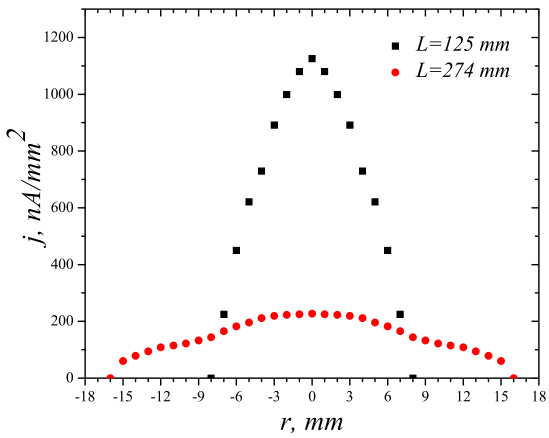

Fig.10. *The ion beam density profiles*

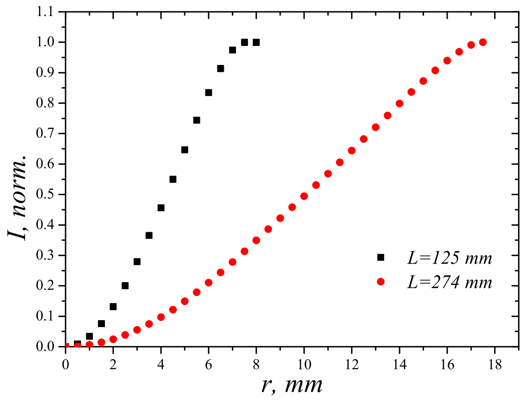

Fig.11. *The ion beam current versus radius*

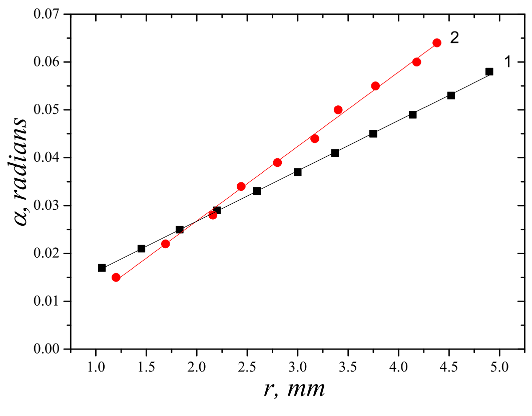

Fig.12. *The half divergence angle versus ion beam radius, 1 - theoretical curve, 2 - experimental data*

The dependence of half angle divergence of ion beam versus ion beam radius is shown in the Fig.12. The curve 2 is experimental data. The radius value was taken on the distance of 90 mm from emission hole. The curve 1 is the analysis result of theoretical calculation of ion beam trajectory for given system of ion beam formation. Small discrepancy between these two functions can be explained by:

- experimental data are averaged because aperture of Faraday cup is 1 mm;
- trajectory calculation are carried out when a step changing of start ion coordinate was set to 0.1 mm; angle between initial trajectory and beam axis has a step changing of 0.5°; energy spread was not taking into account.

The similar measurements were made with extraction voltages equal to: 8, 5 and 2 kV.

The important characteristic of ion beam is energy spread. The energy spectra of ions extracted from the ion source was measured by method of potential inhibition.

The ion energy spread spectra for neon and helium were measured.

For neon ions the energy spectra were studied at constant discharge voltage of 4.3 kV and various operation gas flows: $(2.5\ldots8.9)\cdot10^{-5}\,m^3Pa/s$. The results of experiment are shown in the Fig.13 (A and B). For helium ions the energy spectra were studied when constant discharge voltage was 4.3 kV and value of operation gas flow varies from $2.2\cdot10^{-5}\,m^3Pa/s$ up to $8.9\cdot10^{-5}\,m^3Pa/s$ and when operation gas flow was constant too but various discharge voltages. The results of these experiments are shown in the Fig.14 (A,B) and the Fig.15 (A,B).

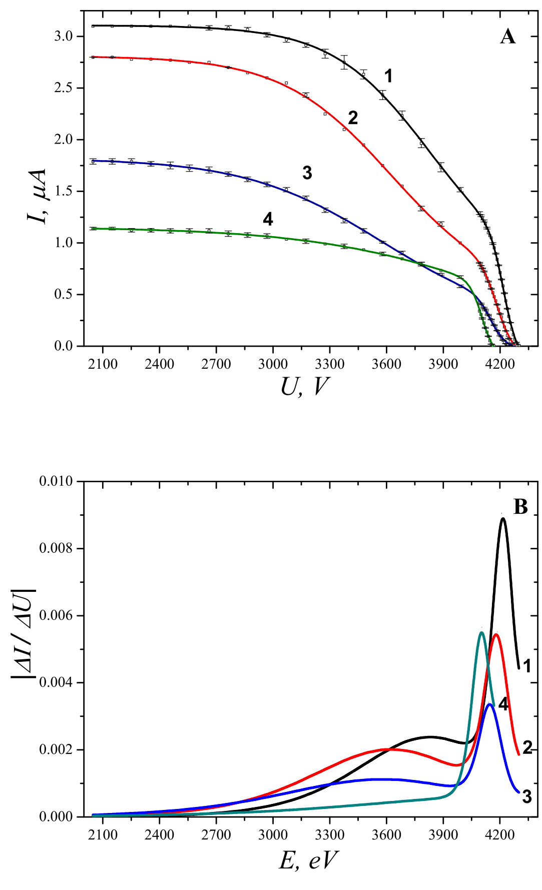

Fig.13. ***A*** *- The Faraday cup's current versus potential inhibition for various operation regimes of MCIS for neon ions.* $U_d = 4.3\,kV$. *The operation gas flow: 1 -* $8.9\cdot10^{-5}\,m^3Pa/s$, $I_d = 1.6\,mA$; *2 -* $7.24\cdot10^{-5}\,m^3Pa/s$, $I_d = 1.2\,mA$; *3 -* $5\cdot10^{-5}\,m^3Pa/s$, $I_d = 0.6\,mA$; *4 -* $2.5\cdot10^{-5}\,m^3Pa/s$, $I_d = 0,3\,mA$. ***B*** *- Corresponding ion energy spread spectra*

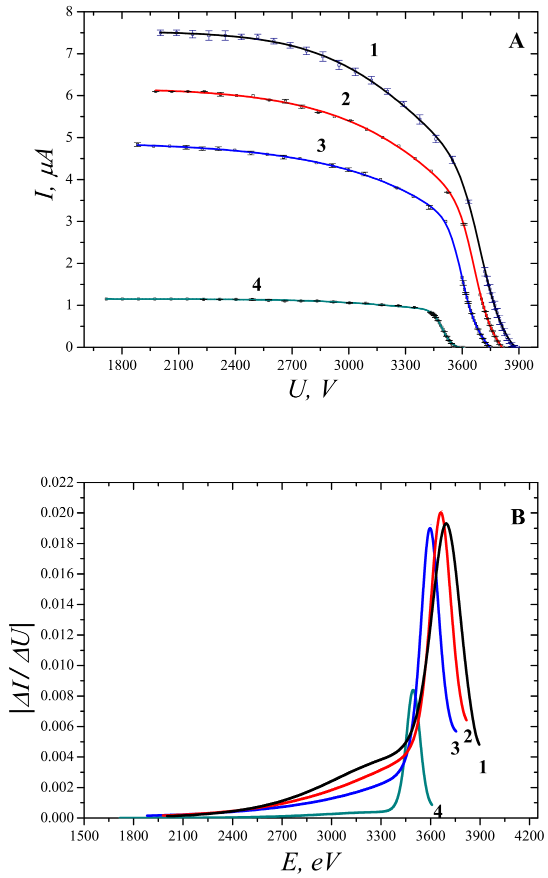

Fig.14. ***A*** *- The Faraday cup's current versus potential inhibition for various operation regimes of MCIS for helium ions.* $U_d = 4.3\,kV$. *The operation gas flow: 1 -* $8.9 \cdot 10^{-5}\,m^3Pa/s$, $I_d = 2.8\,mA$; *2 -* $7.24 \cdot 10^{-5}\,m^3Pa/s$, $I_d = 2.2\,mA$; *3 -* $5 \cdot 10^{-5}\,m^3Pa/s$, $I_d = 1.2mA$; *4 -* $2.2 \cdot 10^{-5}\,m^3Pa/s$, $I_d = 0.6\,mA$. ***B*** *- Corresponding ion energy spread spectra*

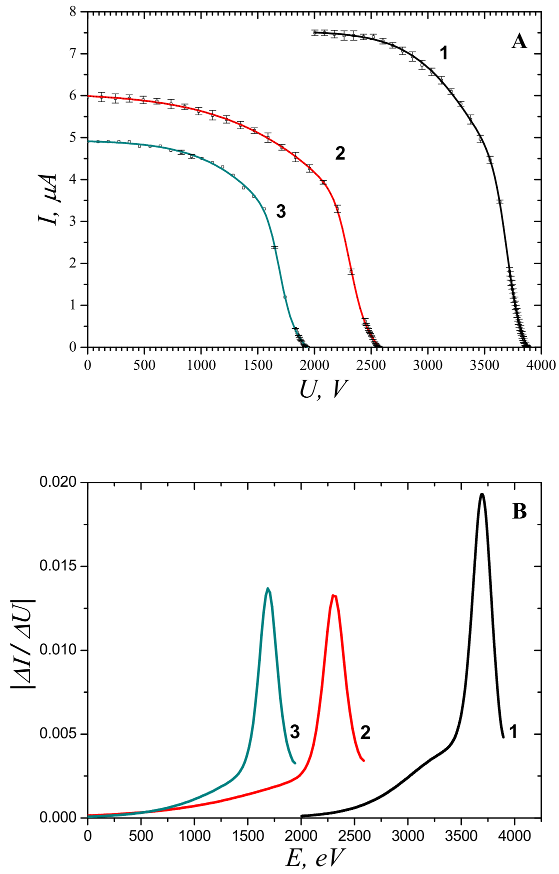

Fig.15. ***A*** *- The Faraday cup's current versus potential inhibition for various operation regimes of MCIS for operation gas flow* $Q = 8.9 \cdot 10^{-5}\,m^3Pa/s$: *1 -*$U_d = 4.3\,kV$, $I_d = 1.6\,mA$; *2 -* $U_d = 3.5\,kV$, $I_d = 2.2\,mA$; *3 -* $U_d = 2.8\,kV$, $I_d = 2.1\,mA$. ***B*** *- Corresponding ion energy spread spectra*

The main characteristics of ion energy distribution namely: E_0- the value of maximum ion energy, E_{max} - the value of ion energy in maximum distribution, ΔE - the ion energy spread (FWHM), are presented in the Table 2 and Table 3.

Table 2.

Neon, U_d=4300 V				
Q·10^{-5}m^{3}Pa/s	8.9	7.24	5	2.5
I_d, mA	1.6	1.2	0.6	0.3
E_0, V	4300	4292	4269	4169
E_{max}, eV	4217	4181	4151	4103
E_0/U_a,	1	0.998	0.99	0.97
E_{max}/U_d,	0.98	0.97	0.96	0.95
ΔE, eV	160	182	188	144
ΔE/E_{max},%	3.8	4.3	4.4	3.5
Helium, U_d=4300 V				
Q·10^{-5}m^{3}Pa/s	8.9	7.24	5	2.2
I_d, mA	2.8	2.2	1.2	0.6
E_0, V	3896	3818	3755	3582
E_{max}, eV	3694	3662	3599	3495
E_0/U_a	0.92	0.88	0.87	0.83
E_{max}/U_d	0.86	0.85	0.83	0.81
ΔE, eV	250	185	163	99
ΔE/E_{max},%	6.75	5	4.5	2.8

Table 3.

U_d, kV	4.3	3.5	2.8
Helium, Q=8.9·10^{-5}m^{3}Pa/s			
I_d, mA	2.8	2.2	2.1
E_0, V	3896	2586	1943
E_{max}, eV	3694	2312	1686
E_0/U_a	0.92	0.74	0.69
E_{max}/U_d	0.86	0.66	0.6
ΔE, eV	250	278	241
ΔE/E_{max},%	6.75	12	14.3

CONCLUSIONS

1. The multi-charge ion source (MCIS) for "SOKOL" accelerator facility was developed.
2. The bench tests of MCIS were made:
2.1. The operation parameters have been determined:

- the range of discharge voltage is $(0\ldots5)\,kV$;
- the range of operation gas flow: $(1.4\ldots8.9)\cdot10^{-5}\,m^3Pa/s$ which depends on operation gas sort and value of extraction ion currents;
- the discharge current: $0\ldots5\,mA$;

2.2. The total ion current and multi-charged ion currents as functions of MCIS operation parameters were studied

(discharge voltage, value of operation gas flow).
2.3. It is shown that MCIS operation parameters and ion beam characteristics are satisfied to exploitation conditions on the "SOKOL" accelerator.
2.4. Main processes of multiply charged ion production are single electron-ion collisions.
3. The initial beam characteristics of ion beam, like maximum divergence angle and ion energy spread, were studied. It is shown that ion energy spread is depends on discharge voltage, sort of operation gas, discharge current. Next regularities were determined:

– with increasing of gas pressure in the ion source and the discharge current too the maximum value of ion energy(E_0) is increasing, and maximum of energy distribution (E_{max}) is tending to the discharge voltage value;

– if the source works with helium in the same field of flow range as for neon then a ratio of maximum ion energy (E_0) and energy (E_{max}) in distribution peak to discharge voltage (U_d) (i.e. E_0/U_d and E_{max}/U_d) are less than for neon but value of discharge current is greater;

– the FWHM of ion energy distribution (ΔE) and ratio $\Delta E/E_{max}$ for helium ions increase with increasing of operation gas flow, but for neon ions the negligible change these values are observed. It can be coupled with present operation parameters of ion source for neon flow when E_{max} is close to U_d;

– for helium ions when helium gas flow is constant and the discharge voltage is changing the values E_0/U_d and $Emax/U_d$ increase with increasing of U_d, but the value $\Delta E/E_{max}$ decreases.

References

1. V.N. Bondarenko, L.S. Glazunov, A.V. Goncharov, A.V. Zats, V.V. Kuz'menko, V.V. Levenets, A.P. Omel'nik, V.M. Pistryak, V.I. Sukhostavetz, A.A. Schur. The analytical nuclear physical complex "Sokol" // *The transactions of XVI International conference of Electrostatic Accelerators and beam technology. Obninsk, Russian Federation* 2007, p. 98-107.

2. Ian G. Brown. *The Physics and Technology of Ion Sources: Second, Revised and Extended Edition.* Weinheim, Wiley-VCH Verlag and KGaA, 2004, 379 p.

3. Atomic & Molecular Numerical Databases of National Institute for Fusion Science https://dbshino.nifs.ac.jp/

4. H. Baumann, K. Bethge. PIG ion source with end extraction for multiply charged ions //*NIM.* 1974, №122, p.517-525.

5. V.V. Kuz'menko, V.M. Pistrak, A.V. Symonenko, Yu. Z. Levchenko. The injector of multiply charged ions for electrostatic accelerator// *VANT. Series: General and Nuclear Physics*. 1983. №24, p.35-38.

6. B.L. Schram, A. J. H. Boerboom, J. Kistemaker. Partial ionization cross sections of noble gases for electrons with energy 0.5-16 keV //*Physica.* 1966, №32, p.185-196, p.197-200.

ИСТОЧНИК МНОГОЗАРЯДНЫХ ИОНОВ

Л.С. Глазунов, А.В. Зац, С.Г. Карпусь, В.В. Кузьменко, В.М. Пистряк

Разработан источник многозарядных ионов (ИМИ) с высоковольтным разрядом Пеннинга и продольным извлечением ионов. Проведены стендовые испытания источника, определены рабочие параметры и первичные характеристики извлекаемого пучка. Показано, что рабочие параметры ИМИ и характеристики извлекаемого пучка удовлетворяют требованиям эксплуатации на ускорителе "СОКОЛ".

ДЖЕРЕЛО БАГАТОЗАРЯДНИХ ІОНІВ

Л.С. Глазунов, А.В. Зац, С.Г. Карпусь, В.В. Кузьменко, В.М. Пістряк

Розроблено джерело багатозарядних іонів (ДБІ) з високовольтним розрядом Пеннінгу та аксіальним витягуванням іонів. Проведені стендові випробування джерела, визначені робочі параметри та первинні характеристики витягнутого пучка. Показано, що робочі параметри ДБІ та характеристики витягнутого пучка задовольняють вимогам експлуатації на прискорювачі "СОКОЛ".